



# DIGITAL ACCESS TO SCHOLARSHIP AT HARVARD

## Systems analysis of the CO<sub>2</sub> concentrating mechanism in cyanobacteria

The Harvard community has made this article openly available.  
[Please share](#) how this access benefits you. Your story matters.

<b>Citation</b>	Mangan, Niall M., and Michael P Brenner. 2014. "Systems analysis of the CO <sub>2</sub> concentrating mechanism in cyanobacteria." eLife 3 (1): e02043. doi:10.7554/eLife.02043. <a href="http://dx.doi.org/10.7554/eLife.02043">http://dx.doi.org/10.7554/eLife.02043</a> .
<b>Published Version</b>	<a href="https://doi.org/10.7554/eLife.02043">doi:10.7554/eLife.02043</a>
<b>Accessed</b>	February 16, 2015 12:24:38 PM EST
<b>Citable Link</b>	<a href="http://nrs.harvard.edu/urn-3:HUL.InstRepos:12406910">http://nrs.harvard.edu/urn-3:HUL.InstRepos:12406910</a>
<b>Terms of Use</b>	This article was downloaded from Harvard University's DASH repository, and is made available under the terms and conditions applicable to Other Posted Material, as set forth at <a href="http://nrs.harvard.edu/urn-3:HUL.InstRepos:dash.current.terms-of-use#LAA">http://nrs.harvard.edu/urn-3:HUL.InstRepos:dash.current.terms-of-use#LAA</a>

*(Article begins on next page)*

# Systems analysis of the CO<sub>2</sub> concentrating mechanism in cyanobacteria

Niall M Mangan<sup>†\*</sup>, Michael P Brenner<sup>\*</sup>

School of Engineering and Applied Sciences and Kavli Institute for Bionano Science and Technology, Harvard University, Cambridge, United States

**Abstract** Cyanobacteria are photosynthetic bacteria with a unique CO<sub>2</sub> concentrating mechanism (CCM), enhancing carbon fixation. Understanding the CCM requires a systems level perspective of how molecular components work together to enhance CO<sub>2</sub> fixation. We present a mathematical model of the cyanobacterial CCM, giving the parameter regime (expression levels, catalytic rates, permeability of carboxysome shell) for efficient carbon fixation. Efficiency requires saturating the RuBisCO reaction, staying below saturation for carbonic anhydrase, and avoiding wasteful oxygenation reactions. We find selectivity at the carboxysome shell is not necessary; there is an optimal non-specific carboxysome shell permeability. We compare the efficacy of facilitated CO<sub>2</sub> uptake, CO<sub>2</sub> scavenging, and HCO<sub>3</sub><sup>-</sup> transport with varying external pH. At the optimal carboxysome permeability, contributions from CO<sub>2</sub> scavenging at the cell membrane are small. We examine the cumulative benefits of CCM spatial organization strategies: enzyme co-localization and compartmentalization.

DOI: [10.7554/eLife.02043.001](https://doi.org/10.7554/eLife.02043.001)

\*For correspondence: [niallmm@gmail.com](mailto:niallmm@gmail.com) (NMM); [brenner@seas.harvard.edu](mailto:brenner@seas.harvard.edu) (MPB)

**Present address:** <sup>†</sup>Mechanical Engineering/LMP, Massachusetts Institute of Technology, Cambridge, MA, United States

**Competing interests:** The authors declare that no competing interests exist.


**Funding:** See page 14

**Received:** 11 December 2013

**Accepted:** 12 April 2014

**Published:** 29 April 2014

**Reviewing editor:** Ron Milo, Weizmann Institute for Science, Israel

 Copyright Mangan and Brenner. This article is distributed under the terms of the [Creative Commons Attribution License](https://creativecommons.org/licenses/by/4.0/), which permits unrestricted use and redistribution provided that the original author and source are credited.

## Introduction

Intracellular compartments are critical for directing and protecting biochemical reactions. One of the simplest and most striking known examples of compartmentalization are the carboxysomes (*Cannon et al., 2001; Yeates et al., 2008*) of cyanobacteria and other autotrophic proteobacteria (*Savage et al., 2010; Rosgaard et al., 2012*). These small, 100–200 nm compartments separate the principal reaction of the Calvin cycle, the RuBisCO catalyzed fixation of carbon dioxide (CO<sub>2</sub>) into 3-phosphoglycerate, from the rest of the cell (*Cannon et al., 1991*). CO<sub>2</sub> and oxygen (O<sub>2</sub>) competitively bind as substrates of RuBisCO, and the reaction with O<sub>2</sub> produces phosphoglycolate, a waste product which must be recycled by the cell (*Jordan and Ogren, 1981; Tcherkez et al., 2006; Savir et al., 2010*). To maximize carboxylation and minimize oxygenation, the carboxysome is believed to act as a diffusion barrier to CO<sub>2</sub> (*Reinhold et al., 1989; Dou et al., 2008*). There is much interest in the design and function of such compartments and whether they can be used to enhance carbon fixation in other organisms such as plants or to improve reaction rates in other metabolic systems (*Papapostolou and Howorka, 2009; Agapakis et al., 2012; Ducat and Silver, 2012; Frank et al., 2013*). Increased efficiency of biochemical reactions will lead to better yield in bioengineered bacterial systems, creating new possibilities for production of high-value products such as biofuels. Enhancing carbon fixation in plants or other organisms could lead to increased carbon sequestration, or crop yield.

The concentrating mechanism in cyanobacteria relies on the interaction of a number of well characterized components, as shown in *Figure 1*, transferring inorganic carbon from outside the cell into cytosol and carboxysomes (*Allen, 1984; Kaplan and Reinhold, 1999; Badger and Price, 2003; Price et al., 2007*). Due to this mechanism, inorganic carbon concentration is elevated well above 200–300 μM, the CO<sub>2</sub> concentration required for saturating the RuBisCO. Additionally a high CO<sub>2</sub> concentration increases the ratio of CO<sub>2</sub> to O<sub>2</sub> so that carboxylation dominates over oxygenation. Concentrations of 20–40 mM inorganic carbon, up to 4000-fold higher than external levels, have been observed (*Sultemeyer et al., 1995; Price et al., 1998; Kaplan and Reinhold, 1999; Woodger et al.,*

**eLife digest** Cyanobacteria are microorganisms that live in water and, like plants, they capture energy from the sun to convert carbon dioxide into sugars and other useful compounds. This process—called photosynthesis—releases oxygen as a by-product. Cyanobacteria were crucial in making the atmosphere of the early Earth habitable for other organisms, and they created the vast carbon-rich deposits that now supply us with fossil fuels. Modern cyanobacteria continue to sustain life on Earth by providing oxygen and food for other organisms, and researchers are trying to bioengineer cyanobacteria to produce alternative, cleaner, fuels.

Understanding how cyanobacteria can be as efficient as possible at harnessing sunlight to ‘fix’ carbon dioxide into carbon-rich molecules is an important step in this endeavor. Carbon dioxide can readily pass through cell membranes, so instead cyanobacteria accumulate molecules of bicarbonate inside their cells. This molecule is then converted back into carbon dioxide by an enzyme found in special compartments within cells called carboxysomes. The enzyme that fixes the carbon is also found in the carboxysomes. However, several important details in this process are not fully understood.

Here, Mangan and Brenner further extend a mathematical model of the mechanism that cyanobacteria use to concentrate carbon dioxide in order to explore the factors that optimize carbon fixation by these microorganisms. Carbon fixation is deemed efficient when there is more carbon dioxide in the carboxysome than the carbon-fixing enzyme can immediately use (which also avoids wasteful side-reactions that use oxygen instead of carbon dioxide). However, there should not be too much bicarbonate, otherwise the enzyme that converts it to carbon dioxide is overwhelmed and cannot take advantage of the extra bicarbonate.

Mangan and Brenner's model based the rates that carbon dioxide and bicarbonate could move in and out of the cell, and the rates that the two enzymes work, on previously published experiments. The model varied the location of the enzymes (either free in the cell or inside a carboxysome), and the rate at which carbon dioxide and bicarbonate could diffuse in and out of the carboxysome (the carboxysome's permeability). Mangan and Brenner found that containing the enzymes within a carboxysome increased the concentration of carbon dioxide inside the cell by an order of magnitude. The model also revealed the optimal permeability for the carboxysome outer-shell that would maximize carbon fixation.

In addition to being of interest to researchers working on biofuels, if the model can be adapted to work for plant photosynthesis, it may help efforts to boost crop production to feed the world's growing population.

DOI: [10.7554/eLife.02043.002](https://doi.org/10.7554/eLife.02043.002)

**2005**). The bilipid outer and cell membranes are highly permeable to small uncharged molecules such as CO<sub>2</sub> (*Gutknecht et al., 1977; Missner et al., 2008*), so instead the cell primarily accumulates the charged and less membrane soluble bicarbonate (HCO<sub>3</sub><sup>-</sup>) (*Volokita et al., 1984; Price and Badger, 1989*). Active transporters, both constitutive and inducible, bring HCO<sub>3</sub><sup>-</sup> into the cell (*Omata et al., 1999; Price et al., 2004, 2008*), and mechanisms exist to actively convert CO<sub>2</sub> to HCO<sub>3</sub><sup>-</sup> at the thylakoid and cell membrane (*Shibata et al., 2001; Maeda et al., 2002; Price et al., 2008*). Once it passively diffuses into the carboxysome, HCO<sub>3</sub><sup>-</sup> is rapidly brought into equilibrium with CO<sub>2</sub> by the enzyme carbonic anhydrase, resulting in the production of CO<sub>2</sub> near RuBisCO. Carbonic anhydrase is known to be localized on the interior side of the carboxysome shell (*Cannon et al., 1991; Cot et al., 2008; Long et al., 2008; Yeates et al., 2008*). The carboxysome shell must be permeable enough to allow HCO<sub>3</sub><sup>-</sup> and 3-phosphoglycerate to readily diffuse in and out. The function of this system and its ability to concentrate inorganic carbon depends on the interplay between these various molecular components. Without a model, flux measurements cannot determine the components relative roles in enhancing the CO<sub>2</sub> concentration in the carboxysome. To date, it has not been possible to directly measure the partitioning of the internal carbon concentration in the cytosol and carboxysomes. We wish to characterize the distribution of internal carbon. Visualizations of the location of the carboxysomes with fluorescent microscopy in *S. elongatus* PCC7942 demonstrated that the carboxysomes are evenly spaced along the centerline of the cell, (*Savage et al., 2010*), raising the question of how spatial organization, beyond simple partitioning, changes the efficacy of the system.

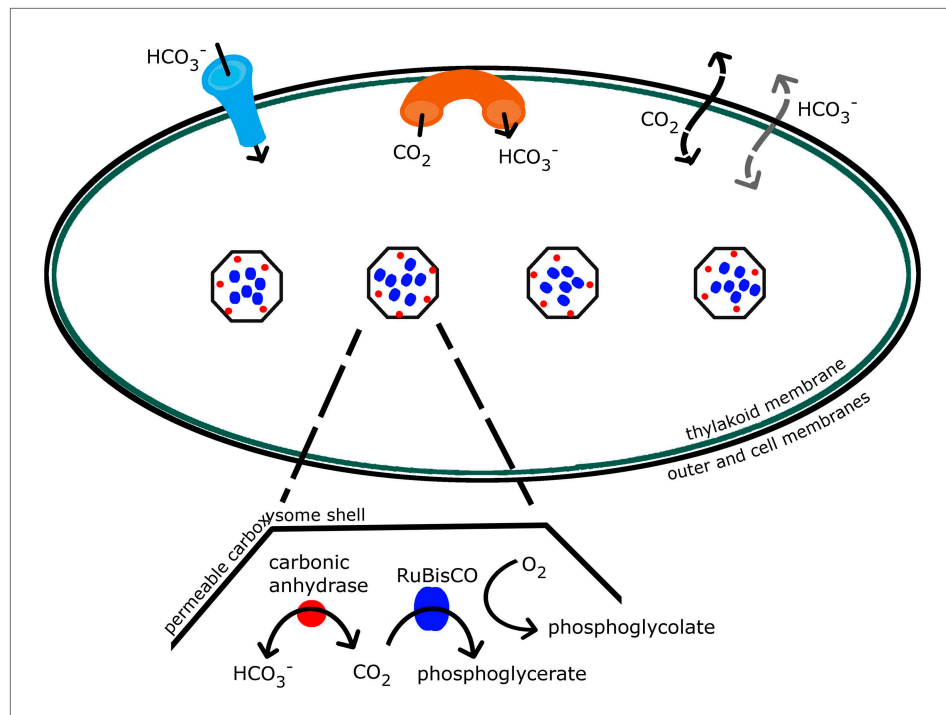


**Figure 1.** Schematic of the CCM in cyanobacteria. Outer and cell membranes (in black), as well as, thylakoid membranes where the light reactions take place (in green) are treated together. Carboxysomes are shown as four hexagons evenly spaced along the centerline of the cell. The model treats a spherically symmetric cell, with one carboxysome at the center. Active  $\text{HCO}_3^-$  transport into the cell is indicated (in light blue), as well as active conversion from  $\text{CO}_2$  to  $\text{HCO}_3^-$  at the membranes, sometimes called ‘facilitated uptake’ or ‘scavenging’ (in orange). Both  $\text{CO}_2$  and  $\text{HCO}_3^-$  can leak in and out of the cell, with  $\text{CO}_2$  leaking out much more readily. Both species passively diffuse across the carboxysome shell. Carbonic anhydrase (red) and RuBisCO (blue) are contained in the carboxysomes and facilitate reactions as shown.

DOI: [10.7554/eLife.02043.003](https://doi.org/10.7554/eLife.02043.003)

The goal of this study is to further develop a mathematical model of the CCM (*Reinhold et al., 1989, 1991; Fridlyand et al., 1996*) that uses recent experimental progress on the CCM to untangle the relative roles of the different molecular components, and predict the region of parameter space where efficient carbon fixation occurs. We are considering conditions where  $\text{CO}_2$  is limiting ( $15 \mu\text{M}$  external inorganic carbon) and, for the moment, ignore other biological pressures. In this context, efficient carbon fixation requires two conditions: First, the  $\text{CO}_2$  concentration must be high enough that RuBisCO is saturated, and the competitive reaction with  $\text{O}_2$  is negligible. We emphasize that for the oxygenation reaction to be negligible the  $\text{CO}_2$  concentration should be higher than needed to merely saturate RuBisCO. Secondly, the carbonic anhydrase within the carboxysome must be unsaturated, so that extra energy isn’t wasted transporting unused  $\text{HCO}_3^-$  into the cell.

Examination of the system performance with varying expression levels of  $\text{HCO}_3^-$  transporters, carboxysome permeability, and conversion from  $\text{CO}_2$  to  $\text{HCO}_3^-$ , reveals a parameter window where these conditions are simultaneously satisfied. We comment on the relation of this window to measured carbon pools, carbon fixation rates, and  $\text{HCO}_3^-$  transporters. We find that the  $\text{HCO}_3^-$  concentration in the cytosol is constant across the cell, set by the  $\text{HCO}_3^-$  transport and leakage rates, and depends very little on the carboxysome permeability. The carboxysome permeability does, however, set how the  $\text{CO}_2$  is partitioned between the carboxysome and cytosol. At optimal carboxysome permeability,  $\text{HCO}_3^-$  diffusion into the carboxysome is fast enough to supply inorganic carbon for fixation, but the rate of  $\text{CO}_2$  leakage out of the carboxysome is low. We explore the fluxes from  $\text{CO}_2$  facilitated uptake and scavenging with varying ratios of external  $\text{CO}_2$  and  $\text{HCO}_3^-$ . Finally we discuss the proportion the carbon concentration comes from different methods of spatial organization such as co-localization, encapsulation, and spatial location of carboxysomes. Concentration of carbonic anhydrase increases

the maximum rate of reaction for carbonic anhydrase per volume, causing carbonic anhydrase to saturate at a higher level of  $\text{HCO}_3^-$ , and achieve an order of magnitude higher local  $\text{CO}_2$  concentrations. Encapsulation of the reactions in an optimally permeable carboxysome shell achieves another order of magnitude of  $\text{CO}_2$  concentration.

## Reaction diffusion model

We present our mathematical model, which captures all aspects of the CCM as described above. This model is an expansion of previously developed models (Reinhold et al., 1989, 1991; Fridlyand et al., 1996). Our three dimensional model of the CCM solves for both the  $\text{HCO}_3^-$  and  $\text{CO}_2$  concentration throughout the a spherical cell. We solve this model numerically and analytically at steady state for three different spatial organizations of carbonic anhydrase and RuBisCO in the cell (Figure 6): enzymes distributed evenly throughout the cell, enzymes localized to the center of the cell but not encapsulated (as they would be on a scaffold), enzymes encapsulated in a carboxysome. We compare the effects of these scenarios in the discussion section, and for now consider a spherical cell of radius  $R_b = 0.5 \mu\text{m}$  with a single spherical carboxysome of radius  $R_c = 50 \text{ nm}$  containing RuBisCO and carbonic anhydrase. Numerical computations are carried out with finite difference methods in MATLAB. The details of analytic solutions are given in the **Supplementary file 1**.

We include the effects of 3D diffusion, active transport and leakage through the cell membrane, and reactions with carbonic anhydrase and RuBisCO. In the carboxysome ( $r < R_c$ ), the equations governing the  $\text{HCO}_3^-$  and  $\text{CO}_2$ , here H and C respectively, are

$$\partial_t C = D\nabla^2 C + R_{CA} - R_{Rub} \quad (1)$$

$$\partial_t H = D\nabla^2 H - R_{CA}, \quad (2)$$

where here  $D$  is the diffusion constant, and  $R_{CA}$  is the carbonic anhydrase reaction, and  $R_{Rub}$  is the RuBisCO reaction. The carbonic anhydrase reactions follows reversible Michaelis–Menten kinetics (Kaplan and Reinhold, 1999; Price et al., 2007),

$$R_{CA}(H, C) = \frac{V_{ba}K_{ca}H - V_{ca}K_{ba}C}{K_{ba}K_{ca} + K_{ca}H + K_{ba}C}, \quad (3)$$

where  $V_{ca}$  and  $V_{ba}$  are hydration and dehydration rates, proportional to the local carbonic anhydrase concentration.  $K_{ca}$  and  $K_{ba}$  are the concentration at which hydration and dehydration are half maximum. The RuBisCO reaction follows Michaelis–Menten kinetics with competitive binding with  $\text{O}_2$ ,  $R_{Rub} = V_{max}C/(C + K_m)$ , where  $K_m = K'_m(1 + O/K_i)$ . Here  $V_{max}$  is the maximum rate of carbon fixation and  $K_m$  is the apparent half maximum concentration value, which has been modified to include competitive binding with  $\text{O}_2$ ,  $O$ .  $K_i$  is the dissociation constant of  $\text{O}_2$  with the RuBisCO and  $K'_m$  is the half maximum concentration with no  $\text{O}_2$  present. RuBisCO also requires ribulose-1,5-bisphosphate, the substrate which  $\text{CO}_2$  reacts with to produce 3-phosphoglycolate. Under  $\text{CO}_2$  limiting conditions it has been shown that there is sufficient ribulose-1,5-bisphosphate to saturate all RuBisCO active sites, and the reaction rates are independent of ribulose-1,5-bisphosphate concentrations (Mayo et al., 1989; Whitehead et al., 2014).

In the cytosol there is no carbonic anhydrase or RuBisCO activity, so  $R_{CA} = 0$  and  $R_{Rub} = 0$ , and there is only diffusion of  $\text{CO}_2$  and  $\text{HCO}_3^-$ . We do not include the natural, but slow, interconversion of  $\text{CO}_2$  and  $\text{HCO}_3^-$  in the cytosol. This assumption is a good one given that the  $\text{HCO}_3^-$  concentration is known to be held out of equilibrium in the cell (Volokita et al., 1984; Price and Badger, 1989). In agreement with this experimental observation, we find that all the other processes effecting the concentration of  $\text{HCO}_3^-$  in the cytosol happen much faster than the natural interconversion.

Boundary conditions proscribe the inorganic carbon fluxes into the cell and the diffusion across the carboxysome boundary. We treat the inorganic carbon fluxes at cell and thylakoid membranes together. At this cell boundary, there is passive leakage of both  $\text{CO}_2$  and  $\text{HCO}_3^-$ : the velocity of  $\text{CO}_2$  across the cell membrane,  $k_m^C$  is about 1000-fold higher than that of  $\text{HCO}_3^-$ ,  $k_m^H$ , due to the lower permeability of the membrane to charged molecules. To account for active import of  $\text{HCO}_3^-$ , we combine the total  $\text{HCO}_3^-$  flux,  $j_c$ , from all  $\text{HCO}_3^-$  transporters. These transporters include BCT1 (encoded by *cpm*), which is thought to be powered by ATP; and BicA and SbtA which are thought to be

symporters between  $\text{HCO}_3^-$  and  $\text{Na}^+$ , driven by the highly controlled electrochemical gradient for  $\text{Na}^+$  (Omata et al., 1999; Price et al., 2004, 2008). Additionally, there are two complexes NDH-1<sub>3</sub> and NDH-1<sub>4</sub> responsible for converting  $\text{CO}_2$  to  $\text{HCO}_3^-$ . This conversion is thought to either decrease  $\text{CO}_2$ , creating a gradient across the membranes and ‘facilitating uptake’ of  $\text{CO}_2$ , or ‘scavenge’  $\text{CO}_2$  which has escaped from the carboxysome. These are localized to the thylakoid and possibly the plasma membrane. They have been linked to the photosynthetic linear and cyclic electron transport chain (Shibata et al., 2001; Maeda et al., 2002; Price et al., 2008). It has been proposed that electron transport drives the formation of local alkaline pockets where  $\text{CO}_2$  more rapidly converts to  $\text{HCO}_3^-$ . We simply describe the conversion with a maximal reaction rate  $\alpha$ , and concentration of half maximal activity of  $K_\alpha$ . Combining these effects, the boundary condition setting diffusive flux of  $\text{HCO}_3^-$  and  $\text{CO}_2$  at the cell membrane is

$$D\partial_r C = -\frac{\alpha C_{\text{cytosol}}}{K_\alpha + C_{\text{cytosol}}} + k_m^C (C_{\text{out}} - C_{\text{cytosol}}) \quad (4)$$

$$D\partial_r H = j_c H_{\text{out}} + \frac{\alpha C_{\text{cytosol}}}{K_\alpha + C_{\text{cytosol}}} + k_m^H (H_{\text{out}} - H_{\text{cytosol}}) \quad (5)$$

where the subscript *cytosol* and *out* indicate we are taking the concentration immediately inside and outside the cell boundary respectively. The diffusion constant times partial derivatives with respect to the radial coordinate,  $r$ , define the diffusive flux at the membrane.

The carboxysome shell is composed of proteins with a radius  $R_c \approx 50$  nm. As of yet, there have been no direct measurements of the carboxysome permeability to small molecules. Using the carboxysome geometry, we can calculate an upper bound for the diffusive velocity across the carboxysome shell, which is directly related to the carboxysome permeability. Crystal structures (Yeates et al., 2007, 2008; Cheng et al., 2008) show the surface has approximately  $N_{\text{pores}} = 4800$  small pores with radius  $r_{\text{pore}} \approx 0.35$  nm, and thickness  $l = 1.8$  nm. If  $k_c$  is the characteristic velocity that small molecules pass through the shell, these numbers imply the upper bound for diffusive transport  $k_c < \frac{\pi r_{\text{pore}}^2 D}{4\pi R_c^2 l} (N_{\text{pores}}) \approx 0.02 \frac{\text{cm}}{\text{s}}$ . This calculation is done by taking the probability that a molecule will encounter a pore on the carboxysome shell  $\left( \frac{N_{\text{pores}} \times \text{pore surface area}}{\text{carboxysome surface area}} \right)$  and multiplying it by the speed

a small molecule will diffuse through the length of the pore ( $D/l$ ). Since it does not take into account any charge effects, which would add an additional energy barrier, it is an upper bound. Although there has been much speculation that the positively charged pores might enhance diffusion of negatively charged  $\text{HCO}_3^-$  (Cheng et al., 2008; Dou et al., 2008; Yeates et al., 2008), here we explore the simplest assumption, that both  $\text{HCO}_3^-$  and  $\text{CO}_2$  have the same permeability. Namely, the boundary conditions at the carboxysome shell are

$$D\partial_r C = k_c (C_{\text{cytosol}} - C_{\text{carboxysome}}) \quad (6)$$

$$D\partial_r H = k_c (H_{\text{cytosol}} - H_{\text{carboxysome}}). \quad (7)$$

We will vary  $k_c$  (henceforth called carboxysome permeability, although it is a velocity) within our model and see that there is a range of  $k_c$  where the CCM is effective even with  $k_c$  identical for  $\text{CO}_2$  and  $\text{HCO}_3^-$ .

## Results

### Analysis of model: finding functional parameter space

Now that we have defined our model, we wish to find the range of parameters where efficient carbon fixation occurs. In what follows, we fix the enzymatic rates, cell membrane permeability, and diffusion constant as reported in the literature (Gutknecht et al., 1977; Jordan and Ogren, 1981; Heinhorst et al., 2006; Missner et al., 2008; Tables 1 and 2). Note that full analytic solutions are available in

**Table 1.** Parameter values chosen for main set of simulations, unless otherwise indicated

Parameter	Definition	Value	Reference
$H_{out}$	concentration of bicarbonate outside the cell	14 $\mu\text{M}^*$	(Price et al., 2008)
$C_{out}$	concentration of carbon dioxide outside of cell	0.14 $\mu\text{M}^*$	(Price et al., 2008)
$D$	diffusion constant of small molecules, $\text{CO}_2$ and $\text{HCO}_3^-$	$10^{-5} \frac{\text{cm}^2}{\text{s}}$	(Fridlyand et al., 1996)
$k_m^C$	permeability of cell membrane to $\text{CO}_2$	$0.3 \frac{\text{cm}}{\text{s}}$	(Gutknecht et al., 1977; Missner et al., 2008)
$k_m^H$	permeability of cell membrane to $\text{CO}_2$	$3 \times 10^{-4} \frac{\text{cm}}{\text{s}}$	(Gutknecht et al., 1977; Missner et al., 2008)
$R_c$	radius of carboxysome	$5 \times 10^{-6} \text{ cm}$	(Schmid et al., 2006; Cheng et al., 2008)
$R_b$	radius of bacteria	$5 \times 10^{-5} \text{ cm}$	(Savage et al., 2010)
$j_c$	$\text{HCO}_3^-$ transport rate resulting in 30 mM cytosolic $\text{HCO}_3^-$ pool	$0.7 \frac{\text{cm}}{\text{s}}^*$	calculated
$k_c$	optimal carboxysome permeability	$6 \times 10^{-3} \frac{\text{cm}}{\text{s}}^*$	calculated
$V_{cell}$	cell volume	$5.2 \times 10^{-10} \mu\text{L}$	calculated
$SA_{cell}$	cell surface area	$3 \times 10^{-8} \text{ cm}^2$	calculated

\*these parameters are varied in the text, but these values are used unless noted otherwise.

DOI: [10.7554/eLife.02043.004](https://doi.org/10.7554/eLife.02043.004)

**Supplementary file 1** sections S3 and S4, so the effect of varying these parameters can be analyzed. We consider the efficacy of the CCM as a function of  $j_c$ , the flux of  $\text{HCO}_3^-$  into the cell,  $k_c$ , the carboxysome permeability, and the parameters ( $\alpha$ ,  $K_a$ ) governing the  $\text{CO}_2$  facilitated uptake mechanism. Both  $\alpha$  and  $j_c$  can be regulated by the organism and vary depending on environmental conditions, whereas the carboxysome permeability,  $k_c$ , is the parameter with the largest uncertainty and debate (Cannon et al., 2001; Cheng et al., 2008; Yeates et al., 2008).

For any given pair of  $k_c$  and  $j_c$ , we ask whether the  $\text{CO}_2$  concentrating mechanism is effective, using the criteria of saturating RuBisCO, reducing oxidation reactions, and not increasing the  $\text{HCO}_3^-$  concentration beyond carbonic anhydrase saturation. Our central result is presented in **Figure 2**, which shows the range of  $k_c$  and  $j_c$  where these conditions are met, assuming that there is no facilitated uptake,  $\alpha = 0$ . The blue shaded region shows where RuBisCO is unsaturated, and the red shaded region shows where carbonic anhydrase is saturated. There is a crescent shaped region between these regions, where the CCM is effective according to our criteria. In the white region oxygenation

**Table 2.** Table comparing enzymatic rates (Sultemeyer et al., 1995; Woodger et al., 2005; Heinhorst et al., 2006)

Enzyme reaction	active sites	$k_{cut} \left[ \frac{1}{\text{s}} \right]$	$V_{max} \text{ in cell} \left[ \frac{\mu\text{M}}{\text{s}} \right]$	$V_{max} \text{ in carboxysome} \left[ \frac{\mu\text{M}}{\text{s}} \right]$	$K_{1/2} [\mu\text{M}]$
carbonic anhydrase hydration	80	$8 \times 10^4$	$1.1 \times 10^4$	$2 \times 10^8$	$3.2 \times 10^3$
carbonic anhydrase dehydration	80	$4.6 \times 10^4$	$9.5 \times 10^4$	$1.7 \times 10^8$	$9.3 \times 10^3$
RuBisCO carboxylation	2160	26	103	$1.7 \times 10^6$	270

$V_{max}$  in cell and carboxysome refer to the volumetric reaction rate assuming the enzymes are distributed throughout the entire cell or only carboxysome.  $V_{ba}$  ( $V_{max}$  for carbonic anhydrase dehydration) is estimated by assuming  $K_{eq} = 5$  and using parameters found in Heinhorst et al. (2006).  $V_{ca}$  is  $V_{max}$  for carbonic anhydrase hydration. Similarly,  $K_{ba}$ , and  $K_{ca}$  are  $K_{1/2}$  for dehydration and hydration respectively.

DOI: [10.7554/eLife.02043.005](https://doi.org/10.7554/eLife.02043.005)

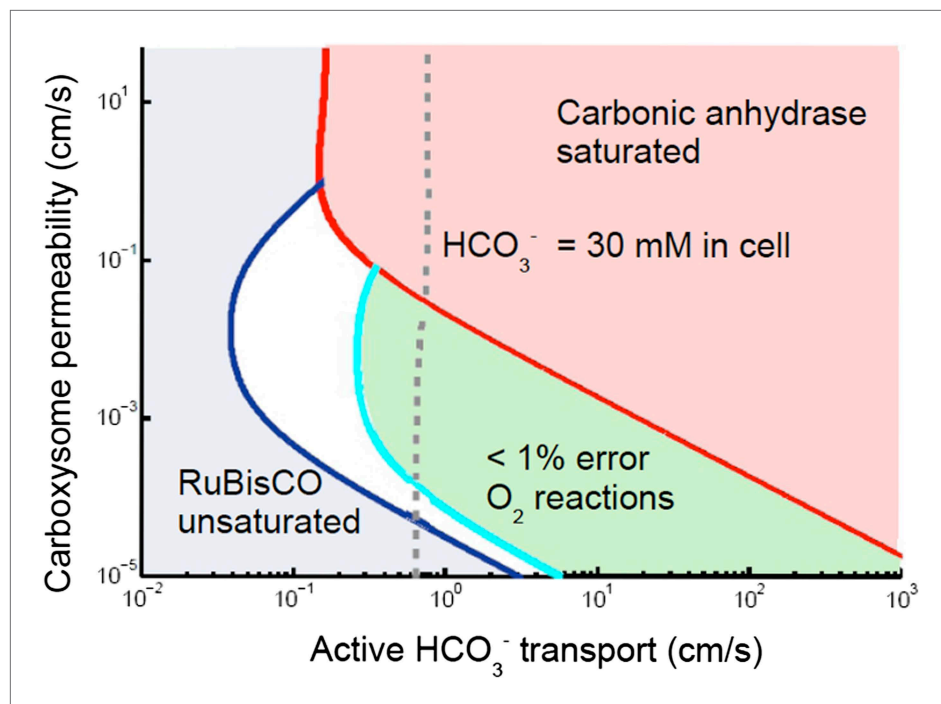


**Figure 2.** Phase space for  $\text{HCO}_3^-$  transport,  $j_a$  and carboxysome permeability  $k_c$ . Plotted are the parameter values at which the  $\text{CO}_2$  concentration reaches some critical value. The left most line (dark blue) indicates for what values of  $j_c$  and  $k_c$  the  $\text{CO}_2$  concentration in the carboxysome would half-saturate RuBisCO ( $K_m$ ). The middle line (light blue) indicates the parameter values which would result in a  $\text{CO}_2$  concentration where 99% of all RuBisCO reactions are carboxylation reactions and only 1% are oxygenation reactions when  $\text{O}_2$  concentration is  $260 \mu\text{M}$ . The right most (red) line indicates the parameter values which result in carbonic anhydrase saturating. Here  $\alpha = 0$ , so there is no  $\text{CO}_2$  scavenging or facilitated uptake. The dotted line (grey) shows the  $k_c$  and  $j_c$  values, where the  $\text{HCO}_3^-$  concentration in the cytosol is 30 mM. The  $\text{HCO}_3^-$  concentration in the cytosol does not vary appreciably with  $k_c$  in this parameter regime, and reaches 30 mM at  $j_c \approx 0.7 \frac{\text{cm}}{\text{s}}$ . All other parameters, such as reaction rates are held fixed and the value can be found in the **Table 1 and 2**.<sup>5</sup>

DOI: [10.7554/eLife.02043.006](https://doi.org/10.7554/eLife.02043.006)

The following figure supplements are available for figure 2:

**Figure supplement 1.** Phase space for  $\text{HCO}_3^-$  transport and carboxysome permeability.

DOI: [10.7554/eLife.02043.007](https://doi.org/10.7554/eLife.02043.007)

**Figure supplement 2.** Effect of  $\text{CO}_2$  scavenging or facilitated uptake on phase space for  $\text{HCO}_3^-$  transport,  $j_a$  and carboxysome permeability,  $K_c$ .

DOI: [10.7554/eLife.02043.008](https://doi.org/10.7554/eLife.02043.008)

reactions happen at a rate of greater than 1%. In the green shaded region oxygenation reactions occur at a rate of less than 1%. Within the white and green regions the  $\text{CO}_2$  concentration in the carboxysome varies greatly.

The lines dividing the regions in **Figure 2** are lines of constant carboxysomal  $\text{CO}_2$  concentration in  $j_c$  and  $k_c$  parameter space. The dark blue line is where  $\text{CO}_2 = K_m$ , the  $\text{CO}_2$  concentration for half maximum RuBisCO reactions. The light blue line indicates parameter values resulting in the  $\text{CO}_2$  concentration ( $C_{99\%}$ ) where rate of oxygenation reactions is 1% for  $\text{O}_2$  concentration of  $260 \mu\text{M}$ . Varying carboxysome permeability,  $k_c$  values, require more or less  $\text{HCO}_3^-$  transport,  $j_c$ , to achieve the same carboxysomal  $\text{CO}_2$  concentration.

We can calculate an amplification factor for the  $C_{99\%}$  line of constant carboxysomal  $\text{CO}_2$  concentration as  $A_C = \frac{C_{\text{carboxysome}}}{C_{\text{out}} + H_{\text{out}}} = 133$ . Any combination of  $j_c$  and  $k_c$  which produce  $C = C_{99\%}$ , make 133 times more  $\text{CO}_2$  available in the carboxysome than there is total inorganic carbon outside the cell. Generally, increasing  $\text{HCO}_3^-$  transport, below the carbonic anhydrase saturation point results in higher  $\text{CO}_2$  concentration in the carboxysome.



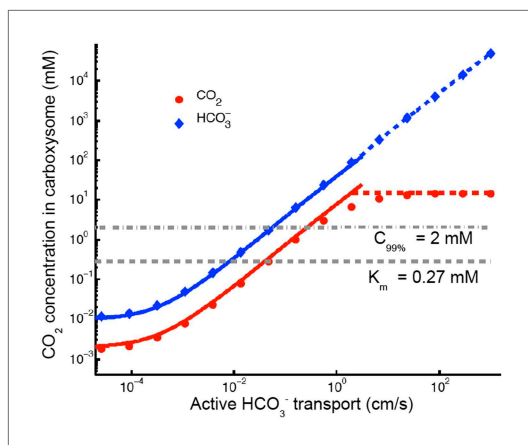


**Figure 3.** Numerical solution (diamonds and circles) and analytic solutions (carbonic anhydrase unsaturated, solid lines, and saturated, dashed lines) correspond well.  $\text{HCO}_3^-$  transport is varied, and all other system parameters are held constant. The  $\text{CO}_2$  concentration above which RuBisCO is saturated is  $K_m$  (grey dashed line). The  $\text{CO}_2$  concentration where the oxygen reaction error rate will be 1% is  $C_{99\%}$  (grey dash-dotted line). The transition between carbonic anhydrase being unsaturated and saturated happens where the two analytic solutions meet (where the dashed and solid red lines meet). Below a critical value of transport,  $j_c \approx 1e^{-3} \frac{\text{cm}}{\text{s}}$  the level of transport is lower than the  $\text{HCO}_3^-$  leaking through the cell membrane.

DOI: [10.7554/eLife.02043.009](https://doi.org/10.7554/eLife.02043.009)

The following figure supplements are available for figure 3:

**Figure supplement 1.** No effect of localizing carbonic anhydrase to the shell of the carboxysome.

DOI: [10.7554/eLife.02043.010](https://doi.org/10.7554/eLife.02043.010)

regime occurs in **Figure 3** when  $H_{\text{carboxysome}} > K_{\text{ba}}$ , so that increasing  $H_{\text{carboxysome}}$  (controlled directly by  $j_d$ ) no longer increases the rate of production of  $C_{\text{carboxysome}}$ . This transition from unsaturated to saturated carbonic anhydrase defines the line for the carbonic anhydrase saturated region in **Figure 2**.

### Carboxysome permeability has optimal value

For each line of constant concentration in **Figure 2** there is an optimal permeability value, where the least  $\text{HCO}_3^-$  transport is required to achieve the same  $\text{CO}_2$  concentration. The optimal permeability value shifts downward with increasing  $\text{CO}_2$  concentration (compare light and dark blue curves). For  $C_{99\%}$  the optimal permeability is  $k_c = 6 \times 10^{-3} \frac{\text{cm}}{\text{s}}$ , below the calculated upper bound:  $k_c < 0.02 \frac{\text{cm}}{\text{s}}$

obtained above from the carboxysome structure. To further understand the effect of permeability, we examine the  $\text{CO}_2$  concentration in the carboxysome for varying carboxysome permeabilities and a fixed  $\text{HCO}_3^-$  transport rate in **Figure 4**. **Figure 4A**, shows that there is a broad range of  $k_c$  where the CCM has maximal efficacy. **Figure 4** shows the distribution of inorganic carbon throughout the cell when the permeability is low (B), optimal (C), and high (D). At high permeability, the  $\text{CO}_2$  produced in the carboxysome rapidly leaks out of the carboxysome, and the  $\text{CO}_2$  concentration in the cytosol, shown in **Figure 4D**, is relatively high. When the carboxysome permeability decreases to near the optimal value, **Figure 4D**, the carboxysome traps  $\text{CO}_2$ , and the cytosolic levels are lower, decreasing leakage out of the cell. This transition occurs when diffusion across the cell (and carboxysome) takes a shorter time than diffusion through the carboxysome shell; or the  $\text{CO}_2$  in the carboxysome is effectively partitioned from the  $\text{CO}_2$  in the cell.

### Varying $\text{HCO}_3^-$ transport saturates enzymes

The basic physics of the phase diagram **Figure 2** follows from examining how  $\text{CO}_2$  and  $\text{HCO}_3^-$  in the carboxysome change as  $j_c$  is varied. **Figure 3** shows the response to varying  $j_c$  with  $k_c = 6 \times 10^{-3} \frac{\text{cm}}{\text{s}}$  (the optimal value in **Figure 4**).

When  $j_c$  is low, the ratio of  $\text{CO}_2$  and  $\text{HCO}_3^-$  is constant, set by the chemical equilibrium at a given pH. In this case the rate of the carbonic anhydrase reaction is much faster than diffusion within the carboxysome, so that  $V_{\text{ba}}K_{\text{ca}}H = V_{\text{ca}}K_{\text{ba}}C$ . Unlike the uncatalyzed interconversion of  $\text{CO}_2$  and  $\text{HCO}_3^-$  in the cytosol, carbonic anhydrase brings the concentrations in the carboxysome to equilibrium very quickly. The chemical equilibrium is  $K_{\text{eq}} = H/C = (K_{\text{ba}}V_{\text{ca}})/(K_{\text{ca}}V_{\text{ba}}) \approx 5$ , for pH around 7 (**DeVoe and Kistiakowsky, 1961**), so that  $\text{HCO}_3^- > \text{CO}_2$  in the carboxysome. Increased pH would increase  $K_{\text{eq}}$  and the proportion of  $\text{HCO}_3^-$ , while decreased pH would decrease  $K_{\text{eq}}$  and the proportion of  $\text{HCO}_3^-$ . Such variations do not substantially effect the subsequent discussion and mechanisms, although they will change the absolute values of  $\text{CO}_2$  concentration in the carboxysome.

The  $K_m$  dashed line in **Figure 3** shows the  $\text{CO}_2$  level above which RuBisCO reaction is saturated: this gives the RuBisCO saturated (blue) boundary in **Figure 2**. We have similarly marked the concentration  $C_{99\%}$  where there is a 1% oxygen reaction error rate with a dash-dotted line.

At higher levels, the  $\text{CO}_2$  concentration no longer increases with increasing  $j_c$ , because the carbonic anhydrase is saturated. The saturated

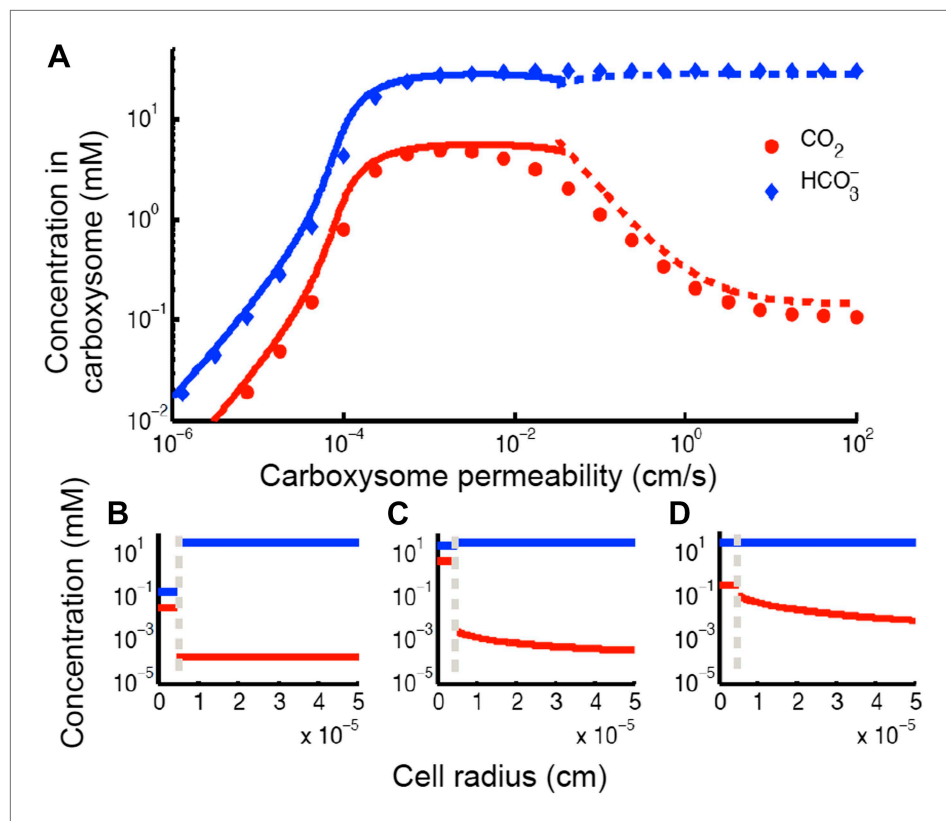


**Figure 4.** Concentration of CO<sub>2</sub> in the carboxysome with varying carboxysome permeability. (A) Numerical solution (diamonds and circles) and analytic solutions (carbonic anhydrase unsaturated, solid lines, and saturated, dashed lines) correspond well. On all plots CO<sub>2</sub> (red circle) < HCO<sub>3</sub><sup>-</sup> (blue diamond). Concentration in the cell along the radius,  $r$ , with carboxysome permeability  $k_c = 1e^{-5} \frac{cm}{s}$  (B),  $k_c = 1e^{-3} \frac{cm}{s}$  (C),  $k_c = 1 \frac{cm}{s}$  (D). Grey dotted lines in (B), (C), (D) indicate location of the carboxysome shell boundary. The transition from low CO<sub>2</sub> at high permeability (D) to maximum CO<sub>2</sub> concentration at optimal permeability (C) occurs at  $k'_c = \frac{D}{R_c} = 2 \frac{cm}{s}$ . At low carboxysome permeability (B) HCO<sub>3</sub><sup>-</sup> diffusion into the carboxysome is slower than consumption. For all subplots  $\alpha = 0 \frac{cm}{s}$  and  $j_c = 0.7 \frac{cm}{s}$ . Qualitative results remain the same with varying  $j_c$ , increasing  $\alpha$  will increase the gradient of CO<sub>2</sub> across the cell as CO<sub>2</sub> is converted to HCO<sub>3</sub><sup>-</sup> at the cell membrane.

DOI: 10.7554/eLife.02043.011

If the carboxysome permeability is below optimal, diffusion of HCO<sub>3</sub><sup>-</sup> into the carboxysome cannot keep up with consumption from RuBisCO. The existence of an optima requires RuBisCO consumption to be low enough that there is a  $k_c$  where the cytosol and carboxysome are partitioned, but HCO<sub>3</sub><sup>-</sup> diffusion in can keep up. When such an optima exists, the carboxysome permeability can improve the CO<sub>2</sub> concentration in the carboxysome without any special selectivity between HCO<sub>3</sub><sup>-</sup> and CO<sub>2</sub>. The location and concentrating power of the optimal regime, is dependent on the size of the cell and the membrane permeabilities to CO<sub>2</sub> and HCO<sub>3</sub><sup>-</sup>.

## Discussion

### Are the fluxes and concentrations reasonable?

While we have solved our model to describe a vast parameters space it is instructive to compare the fluxes and concentrations we find within our optimal parameter space (the green region in **Figure 2**) to actual numbers. At low external inorganic carbon conditions, internal inorganic carbon pools due to CCM activity are regularly measured as high as  $C_i = 30mM$ . The inorganic carbon is predominantly in the form of HCO<sub>3</sub><sup>-</sup>, and measurements do not distinguish between the cytosol and carboxysome

(Sultemeyer et al., 1995; Price et al., 1998, 2008; Kaplan and Reinhold, 1999; Woodger et al., 2005). In our model, we find that the cytosolic  $\text{HCO}_3^-$  concentration is 30 mM when  $j_c = 0.7 \frac{\text{cm}}{\text{s}}$ , over a wide range of the carboxysome permeability (indicated as the dashed grey line in **Figure 2**). From **Figure 4** we can also see that the cytosolic  $\text{HCO}_3^-$  concentration is the dominate form of inorganic carbon in the cell at  $j_c = 0.7 \frac{\text{cm}}{\text{s}}$ . We examine the fate of the  $\text{HCO}_3^-$  transported into the cell in terms of the  $\text{HCO}_3^-$  leaking out,  $\text{CO}_2$  leaking out,  $\text{CO}_2$  fixation or carboxylation, and  $\text{O}_2$  fixation or oxygenation (**Table 3**).

For cells grown under low inorganic carbon conditions net  $\text{HCO}_3^-$  fluxes (transport–leakage) are measured  $10^5 \frac{\text{pmol}}{\text{mgChl s}}$ , with  $\text{CO}_2$  net flux being slightly lower but the same order of magnitude (Badger et al., 1994; Whitehead et al., 2014). High external inorganic carbon conditions produce slightly higher net  $\text{HCO}_3^-$  rates (Tchernov et al., 1997). Assuming chlorophyll per cell volume of around  $10^{-11} \frac{\text{mgChl}}{\text{cell}}$  for cells of our size we can convert this into a flux of  $10^{-6} \frac{\text{pmol}}{\text{cell s}}$  (Keren et al., 2002, 2004; Whitehead et al., 2014). The net  $\text{HCO}_3^-$  flux for our model cell is  $10^{-5} \frac{\text{pmol}}{\text{cell s}}$ , so we are

about an order of magnitude too high. If we choose a  $\text{HCO}_3^-$  transport value one order of magnitude smaller, we will get net fluxes of the same order of magnitude as the measurements at the cost of slightly lower carboxylation rates and higher oxygenation rates (**Table 4**). This would also mean a lower internal  $\text{HCO}_3^-$  pool. Alternatively, the same internal  $\text{HCO}_3^-$  could be reached at a lower flux rate, if the external  $\text{HCO}_3^-$  is higher. We have chosen a dramatically low external inorganic carbon concentration, where the CCM is known to be up-regulated (Price et al., 2008). The general results we present hold until the internal and external concentration are of the same order of magnitude, at which point the CCM is no longer necessary. Since the majority of the  $\text{HCO}_3^-$  transport is balanced by  $\text{HCO}_3^-$  leakage, we can find the transport rate needed to sustain a particular internal concentration by the simple formula:  $j_c = k_m^H (H_{out} - H_{cytosol} (R_b)) / H_{out}$ .

While we can compare the net fluxes, we have not found direct experimental evidence for the absolute  $\text{HCO}_3^-$  uptake rate. To determine whether this  $\text{HCO}_3^-$  transport rate is reasonable we perform a back of the envelope calculation. Our simulated cell has a flux of  $2 \times 10^7$  molecules/s. Assuming the rate of transport per transporter of  $10^3 \frac{\text{molecules}}{\text{s}}$  and our cell's surface area this

**Table 3.** Fate of carbon brought into the cell for  $j_c = 0.7 \text{ cm/s}$  and  $k_c = 6 \times 10^{-3} \text{ cm/s}$

	formula	$\frac{\text{pmol}}{\text{cell s}}$	% of flux
$\text{HCO}_3^-$ transport	$j_c H_{out}$	$3.3 \times 10^{-4}$	
$\text{HCO}_3^-$ leakage	$k_m^H (H_{out} - H_{cytosol} (R_b))$	$3.2 \times 10^{-4}$	96.6
$\text{CO}_2$ leakage	$k_m^C (C_{out} - C_{cytosol} (R_b))$	$10^{-5}$	3.1
carboxylation	$\frac{V_{max} C}{C + K_m \left(1 + \frac{O}{K_o}\right)}$	$9 \times 10^{-7}$	0.3
oxygenation	$\frac{V_{max}^O C}{C + K_m^O \left(1 + \frac{C}{K_c}\right)}$	$3 \times 10^{-9}$	0.001

DOI: 10.7554/eLife.02043.012

**Table 4.** Fate of carbon brought into the cell for  $j_c = 0.07 \text{ cm/s}$  and  $k_c = 6 \times 10^{-3} \text{ cm/s}$

	formula	$\frac{\text{pmol}}{\text{cell s}}$	% of flux
HCO <sub>3</sub> <sup>-</sup> transport	$j_c H_{\text{out}}$	$3.3 \times 10^{-5}$	
HCO <sub>3</sub> <sup>-</sup> leakage	$k_m^H (H_{\text{out}} - H_{\text{cytosol}}(R_b))$	$3.2 \times 10^{-5}$	95.3
CO <sub>2</sub> leakage	$k_m^C (C_{\text{out}} - C_{\text{cytosol}}(R_b))$	$9 \times 10^{-7}$	2.8
carboxylation	$\frac{V_{\text{max}} C}{C + K_m \left(1 + \frac{O}{K_o}\right)}$	$6 \times 10^{-7}$	1.7
oxygenation	$\frac{V_{\text{max}}^O C}{C + K_m^O \left(1 + \frac{C}{K_c}\right)}$	$2 \times 10^{-8}$	0.07

DOI: 10.7554/eLife.02043.013

requires about  $10^3 \frac{\text{transporters}}{\mu\text{m}^2}$ . This is actually not that far off from the number of ATP synthase complexes on the thylakoid membrane in spinach,  $700 \frac{\text{complexes}}{\mu\text{m}^2}$  (Miller and Staehelin, 1979), although it is still quite high.

According to our calculation only around 1 % of the inorganic carbon transported into the cell is fixed into 3-phosphoglycerate. The conclusion that about 99% of inorganic carbon transported into the cell is lost through leakage challenges the assumption that the 3 ATP and 2 NADPH used during the Calvin-Benson-Bassham cycle is the dominant energy expenditure. If it holds true, then cyanobacteria invest much more energy in inorganic carbon uptake than was previously understood. Even in this highly CO<sub>2</sub> concentrating regime,  $5 \times 10^4$  2-phosphoglycolate are produced per second. Cyanobacteria have been shown to have multiple pathways for recycling 2-phosphoglycolate (Hackenberg et al., 2009). Our system fixes CO<sub>2</sub> at a rate of 0.14 pg/hr. Given the volume of our cell, and the fact that between 115–300 fg/μm<sup>3</sup> of carbon are needed to produce a new cyanobacterial cell (Mahlmann et al., 2008) we need between 0.1 and 0.3 picograms of carbon per cell. At the higher flux rate (Table 3) this means that a cell could replicate every 1–2 hr, so faster than cyanobacteria replicate. The lower flux rate (Table 4) would produce fix enough CO<sub>2</sub> for the cell to replicate every 8 to 21 hr, which is similar to the division times of cyanobacteria.

### Concentration profiles of CO<sub>2</sub> and HCO<sub>3</sub><sup>-</sup> across the cell

At  $j_c = 0.7 \frac{\text{cm}}{\text{s}}$ , varying the carboxysome permeability changes how the available inorganic carbon is partitioned between the carboxysome and cytosol, thereby setting the carboxysomal CO<sub>2</sub> concentration as shown in Figure 4. Strikingly, the HCO<sub>3</sub><sup>-</sup> concentration is constant across the cytosol. This is because the cell membranes have low permeability to HCO<sub>3</sub><sup>-</sup>; thus, the rate of escape is slow and HCO<sub>3</sub><sup>-</sup> equilibrates across the cell. A consequence of this flat HCO<sub>3</sub><sup>-</sup> profile is that the carboxysome experiences the same HCO<sub>3</sub><sup>-</sup> concentration, independent of its position in the cell. This means the incoming inorganic carbon source for the carboxysome system is invariant with the position of the carboxysome in the cell.

In contrast, there is a gradient in CO<sub>2</sub> concentration across the cell when the carboxysome permeability is at or above the optimum (Figure 4C,D). The cell membrane is more permeable to CO<sub>2</sub>. The gradient means that the CO<sub>2</sub> leakage out of the cell affects the CO<sub>2</sub> leakage out of the carboxysome. Moving the carboxysome close to the cell membrane increases the leakage rate of CO<sub>2</sub> out of the carboxysome. Notably, in *S. elongatus* the carboxysomes are located along the center line of the cell, away from the cell membranes (Savage et al., 2010). The spatial profiles of HCO<sub>3</sub><sup>-</sup> and CO<sub>2</sub> give no hint as to why the carboxysomes are spaced apart from one another. Since the gradient in HCO<sub>3</sub><sup>-</sup> is flat, there is no competition between the carboxysomes for HCO<sub>3</sub><sup>-</sup> (the main incoming source of

inorganic carbon). In fact, since the local concentration of  $\text{CO}_2$  is higher near a carboxysome, nearby carboxysomes would “feed” each other  $\text{CO}_2$ . As has been shown, such clumping would reduce the probability of distributing carboxysomes equitably to daughter cells, possibly counteracting any benefit (Savage et al., 2010).

The concentration in the carboxysome is basically constant, because the carboxysome is so small that diffusion across it takes very little time. A consequence of this is that the organization of the reactions in the carboxysome does not effect the  $\text{CO}_2$  concentration in the carboxysome (Figure 3—figure supplement 1). Therefore, the localization of the carbonic anhydrase to the inner carboxysome shell seems to have no effect on the CCM. It has been suggested that diffusion in the carboxysome should be slower, since the carboxysome is packed with RuBisCO. One proposed consequence of slower diffusion in the carboxysome is that it could trap  $\text{CO}_2$ , making a low carboxysome permeability unnecessary. We have tested this hypothesis (Figure 2—figure supplement 1), and find that assuming the diffusion constant one would expect for small molecules in a 60% sucrose solution ( $D_c = 10^{-7} \frac{\text{cm}^2}{\text{s}}$ ), does reduce the optimal carboxysome permeability. However, for any carboxysome permeability a higher  $\text{HCO}_3^-$  transport rate is needed to achieve the same carboxysomal  $\text{CO}_2$  concentration. So, if the diffusion is slower in the carboxysome it does not aid the CCM. Even at this slower diffusion, the  $\text{CO}_2$  concentration across the carboxysome is flat.

### Benefit of $\text{CO}_2$ to $\text{HCO}_3^-$ conversion: facilitated uptake or scavenging of $\text{CO}_2$

We investigate the effect of  $\text{CO}_2$  to  $\text{HCO}_3^-$  conversion at the thylakoid and cell membranes (combined in the model). Increasing conversion,  $\alpha > 0$ , can facilitate uptake of  $\text{CO}_2$  from outside the cell and scavenge  $\text{CO}_2$  escaped from the carboxysome. Facilitated uptake results in saturating both carbonic anhydrase and RuBisCO at a lower level of  $\text{HCO}_3^-$  transport. Scavenging broadens the range of carboxysome permeability which will effectively separate the inorganic carbon pools in the carboxysome and outside. Scavenging decreases the concentration of  $\text{CO}_2$  in the cytosol, so a more permeable carboxysome can still result in a low leakage rate of inorganic carbon out of the cell (more of the inorganic carbon in the cytosol is in the form of  $\text{HCO}_3^-$  which leaks out less readily). However, neither of these effects is particularly strong in our current range of reaction rates, and cell membrane permeability (Figure 2—figure supplement 2).

The relative effects of these two mechanisms depends on the external  $\text{CO}_2$  and  $\text{HCO}_3^-$  concentrations. In saltwater environments the pH is near 8 and  $\text{HCO}_3^-$  is the predominant inorganic carbon source. While external pH is not explicitly treated in our model, we can account for changes to pH through the external inorganic carbon concentration. To be consistent with oceanic environment, thus far we have shown results for low external inorganic carbon concentrations of  $[\text{CO}_2] = 0.1 \mu\text{M}$  and  $[\text{HCO}_3^-] = 14.9 \mu\text{M}$ . The effect of facilitated uptake, under these assumptions, is very small. In freshwater or under conditions of ocean acidification, where the pH could fall to 6 or lower, there can be a much larger proportion of  $\text{CO}_2$  (>50%). Figure 5 shows the absolute contribution of  $\text{HCO}_3^-$  transport, facilitated  $\text{CO}_2$  uptake, and  $\text{CO}_2$  scavenging for varying proportions of external  $\text{CO}_2$ . Even though we assume the same velocity of facilitated uptake and  $\text{HCO}_3^-$  transport ( $j_c = \frac{\alpha}{K_a} = 1 \frac{\text{cm}}{\text{s}}$ ), facilitated uptake contributes less because it is limited by  $\text{CO}_2$  diffusion across the membrane. At the same rates of transport the facilitated uptake mechanism only contributes more than active  $\text{HCO}_3^-$  if the  $\text{CO}_2$  concentration is greater than 80% of external inorganic carbon. This is consistent with observations that oceanic cyanobacteria such as Prochlorococcus only seem to possess gene homologs for  $\text{HCO}_3^-$  transport systems, while other freshwater and estuarine cyanobacteria have gene homologs for both constitutive (NDH-1<sub>4</sub>) and inducible (NDH-1<sub>3</sub>)  $\text{CO}_2$  uptake systems as well as inducible  $\text{HCO}_3^-$  transport systems (BicA, SbtA, and BCT1) (Price, 2011).

Scavenging only contributes significantly to total incoming  $\text{HCO}_3^-$  when the carboxysome permeability is higher than optimal, Figure 5, and does not contribute significantly below our calculated upper bound of  $k_c < 0.02 \frac{\text{cm}}{\text{s}}$ . In these ranges for carboxysome permeability, there is very little  $\text{CO}_2$  leaking out of the carboxysome into the cytosol, so there is very little  $\text{CO}_2$  to scavenge, Figure 5. The effect of scavenging is dependent on the cell membrane permeability to  $\text{CO}_2$  and  $\text{HCO}_3^-$ .

Given that scavenging has no obvious affect on  $\text{HCO}_3^-$  concentrations, it is reasonable to wonder why this mechanism exists at all. One might assume that scavenging prevents leakage, but if the energy

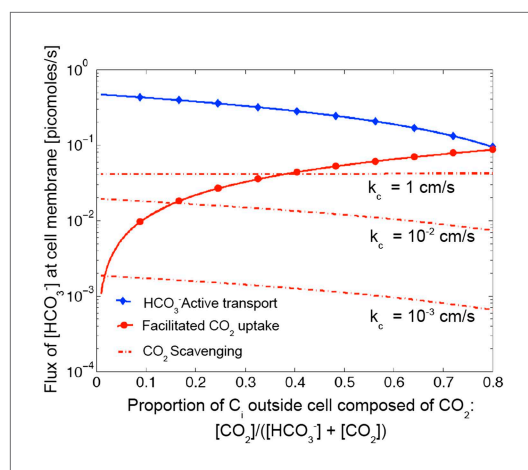


**Figure 5.** Size of the  $\text{HCO}_3^-$  flux in one cell from varying sources, as the proportion of  $\text{CO}_2$  to  $\text{HCO}_3^-$  outside the cell changes. We show results for three carboxysome permeabilities,  $k_c$ , and only the scavenging is effected. Total external inorganic carbon is  $15 \mu\text{M}$ ,  $j_c = 1 \frac{\text{cm}}{\text{s}}$  and  $\frac{\alpha}{K_\alpha} = 1 \frac{\text{cm}}{\text{s}}$ . When the carboxysome permeability is larger than optimal,  $k_c = 1 \frac{\text{cm}}{\text{s}}$ , scavenging can contribute more than facilitated uptake at low external  $\text{CO}_2$  concentrations. However, when the carboxysome permeability at or below our geometric bound,  $k_c \leq 0.02 \frac{\text{cm}}{\text{s}}$ , scavenging is negligibly small. Unless there is very little  $\text{HCO}_3^-$  in the environment,  $\text{HCO}_3^-$  transport seems to be more efficient than  $\text{CO}_2$  facilitated uptake.

DOI: [10.7554/eLife.02043.014](https://doi.org/10.7554/eLife.02043.014)

is gained at the optimal permeability. At optimal carboxysome permeability, the  $\text{CO}_2$  is effectively partitioned into the carboxysome and conversion can act only as facilitated uptake as shown in **Figure 5**.

Another advantage of localizing the enzymes in a small region at the center of the cell is separating carbonic anhydrase from the  $\alpha$  ( $\text{CO}_2$  to  $\text{HCO}_3^-$ ) conversion mechanism, preventing a futile cycle. The futile cycle is most detrimental when the enzymes are distributed throughout the cytosol, and increases the oxygenation error rate by 10% (data not shown). Concentrating the enzymes away from the cell and thylakoid membranes, where conversion happens, removes this effect. With a carboxysome or scaffold the oxygenation rate is almost exactly the same with and without the  $\alpha$  conversion mechanism. This is consistent with the previously shown detrimental effect of having active carbonic anhydrase free within the cytosol (**Price and Badger, 1989**). It would be impossible to keep the cytosol completely free from carbonic anhydrase enzyme, so there must be a way of activating it within the carboxysome only. Carbonic anhydrase is inactivated under reducing conditions (**Peña et al., 2010**). Recently it was shown that carboxysomes oxidize after assembly, providing a way to keep carbonic anhydrase inactive until fully enclosed in a carboxysome (**Chen et al., 2013**).

## Effects of pH

Cyanobacteria must regulate pH as almost all biochemical reactions are pH sensitive. We do not attempt to model this regulation or potential pH variation within the cell, however pH may be included implicitly in a couple ways. We have already explored the effect of varying external pH, and the effects of pH on carbonic anhydrase. Cytosolic pH would have little direct effect on the  $\text{CO}_2$  and  $\text{HCO}_3^-$  levels since the non-enzymatic interconversion is very slow as previously discussed. The effect of internal pH could also be explored by varying the reaction rate of RuBisCO, which is pH sensitive. Varying the reaction rate of RuBisCO greatly could change the range where a non-specific

to bring a 'new'  $\text{HCO}_3^-$  molecule from outside the cell is the same as the energy required to save an 'old'  $\text{CO}_2$  molecule from leaking out, there is no obvious advantage of preventing the leakage. It is possible that since the scavenging mechanism is associated with the electron transport chain of the light reactions of photosynthesis scavenging can be ramped up more easily when there is excess light energy. If this were the case, a comparison of  $j_c = 1 \frac{\text{cm}}{\text{s}}$  and  $\frac{\alpha}{K_\alpha} = 1 \frac{\text{cm}}{\text{s}}$  is deceiving and  $\frac{\alpha}{K_\alpha}$  could be much larger. It has been suggested that the cell uses this mechanism as a way to dissipate excess light energy (**Tchernov et al., 1997, 2003**).

## Cellular organization

The most striking aspect of the CCM is the way that spatial organization is used to increase the efficacy of the reactions. **Figure 6** compares the effect of different enzymatic reaction organizations. Concentrating carbonic anhydrase and RuBisCO to a small region in the center of the cell, on a scaffold for example, leads to an order of magnitude increase in the concentration of  $\text{CO}_2$ . Localizing the carbonic anhydrase to a small volume concentrates it, increasing the maximum reaction rate per volume,  $V_{ca}$  and  $V_{ba}$ . A larger  $V_{ba}$  increases the  $\text{HCO}_3^-$  concentration at which carbonic anhydrase is saturated allowing the mechanism to take advantage of a larger  $\text{HCO}_3^-$  flux,  $j_c$ . A small increase can be gained from encapsulating the enzymes in a permeable carboxysome shell and another order of magnitude

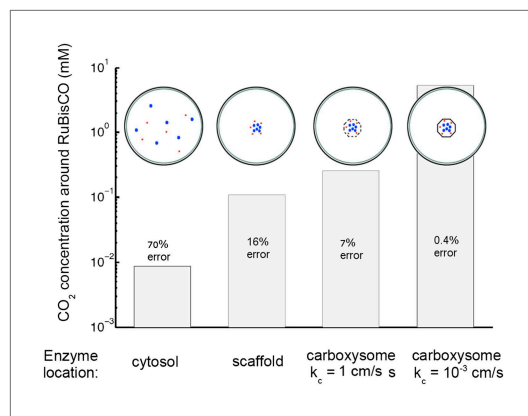


**Figure 6.** Concentration of CO<sub>2</sub> achieved through various cellular organizations of enzymes, where we have selected the HCO<sub>3</sub><sup>-</sup> transport level such that the HCO<sub>3</sub><sup>-</sup> concentration in the cytosol is 30 mM. O<sub>2</sub> concentration is 260 μM. The oxygenation error rates, as a percent of total RuBisCO reactions are indicated on the concentration bars. The cellular organizations investigated are RuBisCO and carbonic anhydrase distributed throughout the entire cytosol, co-localizing RuBisCO and carbonic anhydrase on a scaffold at the center of the cell without a carboxysome shell, RuBisCO and carbonic anhydrase encapsulated in a carboxysome with high permeability at the center of the cell, and RuBisCO and carbonic anhydrase encapsulated in a carboxysome with optimal permeability at the center of the cell.

DOI: [10.7554/eLife.02043.015](https://doi.org/10.7554/eLife.02043.015)

HCO<sub>3</sub><sup>-</sup> concentrations across the cell are flat and are predominately set by the transport rate in, and leakage out. We quantitatively compare the transport rates and concentrations we predict in our optimal parameter space, and find them to be in good agreement with experiment. We also comment on the effects of external pH on CO<sub>2</sub> versus HCO<sub>3</sub><sup>-</sup> uptake mechanisms. Finally we describe the cumulative benefits of co-localization, encapsulation, and optimal carboxysome permeability on the CCM.

Further comparison of this model to experimental flux measurements, especially to determine the quantitative contributions of different transporters under different physiological conditions would be very interesting. Current solutions are for steady state at constant external concentration, but most gas exchange measurements, by necessity, measure the fluxes as the inorganic carbon is depleted in the media. The model could be modified to solve the time dependent problem with varying external inorganic carbon. As of yet the carboxysome permeability has not been measured directly, and it would be quite interesting to see how close it is to our 'optimal' prediction.

## Acknowledgements

We thank Colleen Cavanaugh, Jeremy Gunarawenda and Pam Silver for important conversations. This research was supported by the National Science Foundation through the Harvard Materials Research Science and Engineering Center (DMR-0820484) and the Division of Mathematical Sciences (DMS-0907985). MPB is an Investigator of the Simons Foundation.

## Additional information

### Funding

Funder	Grant reference number	Author
NSF Harvard Materials Research Science and Engineering Center	DMR-0820484	Niall M Mangan, Michael P Brenner

carboxysome permeability can increase the concentration of CO<sub>2</sub> in the carboxysome. It would be unexpected that the RuBisCO rate be much faster than we assume, as we have assumed a rate on the high end. A lower RuBisCO rate would increase the range of effective carboxysome permeabilities. As previously mentioned it has been hypothesized that the CO<sub>2</sub> facilitated uptake mechanism functions by creating local alkaline pockets. Diffusion of hydrogen ions across the cell would be very fast, so it could be very difficult to maintain local alkalinity. Whether such pH gradients are possible, is certainly a subject of future interest.

## Conclusions

We have described and analyzed a model for the CO<sub>2</sub> concentrating mechanism in cyanobacteria. There exists a broad range of HCO<sub>3</sub><sup>-</sup> transport and carboxysome permeability values which result in effective CO<sub>2</sub> concentration in the carboxysome. This effective concentration parameter space is defined by CO<sub>2</sub> levels high enough to saturate RuBisCO and produce a favorable ratio of carboxylation to oxygenation reactions, but not so high as to saturate carbonic anhydrase (after which increasing HCO<sub>3</sub><sup>-</sup> transport will not increase the CO<sub>2</sub> concentration). An optimal, non-specific carboxysome permeability exists, where HCO<sub>3</sub><sup>-</sup> diffusion into the carboxysome is not substantially inhibited, but CO<sub>2</sub> leakage is

Funder	Grant reference number	Author
NSF Division of Mathematical Sciences	DMS-0907985	Niall M Mangan, Michael P Brenner
National Institute of General Medical Sciences	Grant GM068763 for National Centers of Systems Biology	Niall M Mangan, Michael P Brenner

The funders had no role in study design, data collection and interpretation, or the decision to submit the work for publication.

### Author contributions

NMM, Performed calculations, Conception and design, Analysis and interpretation of data, Drafting or revising the article; MPB, Oversaw and mentored research, Conception and design, Drafting or revising the article

## Additional files

### Supplementary file

- Supplementary file 1. Mathematical derivation appendix. Mathematical derivations of analytic solutions for a spherical cell with reactions organized in a variety of ways. We present analytic solutions for the concentration of CO<sub>2</sub> and HCO<sub>3</sub><sup>-</sup> a carboxysome located at the center of the cell. We derive analytic solutions assuming a number of different cases for the enzymatic rates in the carboxysome: RuBisCO reaction rate negligible with carbonic anhydrase saturated and unsaturated, RuBisCO reaction rate non-negligible with carbonic anhydrase unsaturated. Additionally we derive analytic solutions for the enzymatic reactions throughout the cell and localized to a scaffold without a carboxysome shell.

DOI: [10.7554/eLife.02043.016](https://doi.org/10.7554/eLife.02043.016)

## References

- Agapakis CM, Boyle PM, Silver PA. 2012. Natural strategies for the spatial optimization of metabolism in synthetic biology. *Nature Chemical Biology* **8**:527–535. doi: [10.1038/nchembio.975](https://doi.org/10.1038/nchembio.975).
- Allen MM. 1984. Cyanobacterial cell inclusions. *Annual Review of Microbiology* **38**:1–25. doi: [10.1146/annurev.mi.38.100184.000245](https://doi.org/10.1146/annurev.mi.38.100184.000245).
- Badger MR, Palmqvist K, Yu JW. 1994. Measurement of CO<sub>2</sub> and HCO<sub>3</sub><sup>-</sup> fluxes in cyanobacteria and microalgae during steady-state photosynthesis. *Physiologia Plantarum* **90**:529–536. doi: [10.1111/j.1399-3054.1994.tb08811.x](https://doi.org/10.1111/j.1399-3054.1994.tb08811.x).
- Badger MR, Price GD. 2003. CO<sub>2</sub> concentrating mechanisms in cyanobacteria: molecular components and their diversity and evolution. *Journal of Experimental Botany* **54**:609–622. doi: [10.1093/jxb/erg076](https://doi.org/10.1093/jxb/erg076).
- Cannon GC, Bradburne CE, Aldrich HC, Baker SH, Heinhorst S, Shively JM. 2001. Microcompartments in prokaryotes: carboxysomes and related polyhedra. *Applied and Environmental Microbiology* **67**:5351–5361. doi: [10.1128/AEM.67.12.5351-5361.2001](https://doi.org/10.1128/AEM.67.12.5351-5361.2001).
- Cannon GC, English R, Shively JM. 1991. In situ assay of ribulose-1,5-bisphosphate carboxylase/oxygenase in *Thiobacillus neapolitanus*. *Journal of Bacteriology* **173**:1565–1568.
- Chen AH, Robinson-Mosher A, Savage DF, Silver PA, Polka JK. 2013. The bacterial carbon-fixing organelle is formed by shell envelopment of preassembled cargo. *PLOS ONE* **8**:e76127. doi: [10.1371/journal.pone.0076127](https://doi.org/10.1371/journal.pone.0076127).
- Cheng S, Liu Y, Crowley CS, Yeates TO, Bobik TA. 2008. Bacterial microcompartments: their properties and paradoxes. *Bioessays: news and Reviews in Molecular, Cellular and Developmental Biology* **30**:1084–1095. doi: [10.1002/bies.20830](https://doi.org/10.1002/bies.20830).
- Cot S, So AK, Espie GS. 2008. A multiprotein bicarbonate dehydration complex essential to carboxysome function in cyanobacteria. *Journal of Bacteriology* **190**:936–945. doi: [10.1128/JB.01283-07](https://doi.org/10.1128/JB.01283-07).
- DeVoe H, Kistiakowsky GB. 1961. The enzymatic kinetics of carbonic anhydrase from bovine and human erythrocytes. *Journal of the American Chemical Society* **83**:274–280. doi: [10.1021/ja01463a004](https://doi.org/10.1021/ja01463a004).
- Dou Z, Heinhorst S, Williams EB, Murin CD, Shively JM. 2008. CO<sub>2</sub> fixation kinetics of *Halothiobacillus neapolitanus* mutant carboxysomes lacking carbonic anhydrase suggest the shell acts as a diffusional barrier for CO<sub>2</sub>. *The Journal of Biological Chemistry* **283**:10377–10384. doi: [10.1074/jbc.M709285200](https://doi.org/10.1074/jbc.M709285200).
- Ducat D, Silver P. 2012. Improving carbon fixation pathways. *Current Opinion in Chemical Biology* **16**:337–344. doi: [10.1016/j.cbpa.2012.05.002](https://doi.org/10.1016/j.cbpa.2012.05.002).
- Frank S, Lawrence AD, Prentice MB, Warren MJ. 2013. Bacterial microcompartments moving into a synthetic biology world. *Journal of Biotechnology* **163**:273–279. doi: [10.1016/j.jbiotec.2012.09.002](https://doi.org/10.1016/j.jbiotec.2012.09.002).
- Fridlyand L, Kaplan A, Reinhold L. 1996. Quantitative evaluation of the role of a putative CO<sub>2</sub>-scavenging entity in the cyanobacterial CO<sub>2</sub>-concentrating mechanism. *Bio Systems* **37**:229–238. doi: [10.1016/0303-2647\(95\)01561-2](https://doi.org/10.1016/0303-2647(95)01561-2).
- Gutknecht J, Bisson MA, Tosteson FC. 1977. Diffusion of carbon dioxide through lipid bilayer membranes: effects of carbonic anhydrase, bicarbonate, and unstirred layers. *The Journal of General Physiology* **69**:779–794. doi: [10.1085/jgp.69.6.779](https://doi.org/10.1085/jgp.69.6.779).



- Hackenberg C**, Engelhardt A, Matthijs HCP, Wittink F, Bauwe H, Kaplan A, Hagemann M. 2009. Photorespiratory 2-phosphoglycolate metabolism and photoreduction of O<sub>2</sub> cooperate in high-light acclimation of *Synechocystis* sp. strain PCC 6803. *Planta* **230**:625–637. doi: [10.1007/s00425-009-0972-9](https://doi.org/10.1007/s00425-009-0972-9).
- Heinhorst S**, Williams EB, Cai R, Murin CD, Shively JM, Cannon GC. 2006. Characterization of the carboxysomal carbonic anhydrase CsoSCA from *Halothiobacillus neapolitanus*. *Journal of Bacteriology* **188**:8087–8094. doi: [10.1128/JB.00990-06](https://doi.org/10.1128/JB.00990-06).
- Jordan DB**, Ogren WL. 1981. Species variation in the specificity of ribulose biphosphate carboxylase/oxygenase. *Nature* **291**:513–515. doi: [10.1038/291513a0](https://doi.org/10.1038/291513a0).
- Kaplan A**, Reinhold L. 1999. CO<sub>2</sub> concentrating mechanisms in photosynthetic microorganisms. *Annual Review of Plant Physiology and Plant Molecular Biology* **50**:539–570. doi: [10.1146/annurev.arplant.50.1.539](https://doi.org/10.1146/annurev.arplant.50.1.539).
- Keren N**, Aurora R, Pakrasi HB. 2004. Critical roles of bacterioferritins in iron storage and proliferation of cyanobacteria. *Plant Physiology* **135**:1666–1673. doi: [10.1104/pp.104.042770](https://doi.org/10.1104/pp.104.042770).
- Keren N**, Kidd MJ, Penner-Hahn JE, Pakrasi HB. 2002. A light-dependent mechanism for massive accumulation of manganese in the photosynthetic bacterium *Synechocystis* sp. PCC 6803. *Biochemistry* **41**:15085–15092. doi: [10.1021/bi026892s](https://doi.org/10.1021/bi026892s).
- Long BM**, Badger MR, Whitney SM, Price GD. 2008. Analysis of carboxysomes from *Synechococcus* PCC7942 reveals multiple RuBisCO complexes with carboxysomal proteins CcmM and CcaA. *The Journal of Biological Chemistry* **292**:29323–29335. doi: [10.1074/jbc.M703896200](https://doi.org/10.1074/jbc.M703896200).
- Maeda S**, Badger MR, Price GD. 2002. Novel gene products associated with NdhD3/D4-containing NDH-1 complexes are involved in photosynthetic CO<sub>2</sub> hydration in the cyanobacterium, *Synechococcus* sp. strain PCC7942. *Molecular Microbiology* **43**:425–435. doi: [10.1046/j.1365-2958.2002.02753.x](https://doi.org/10.1046/j.1365-2958.2002.02753.x).
- Mahlmann DM**, Jahnke J, Loosen P. 2008. Rapid determination of the dry weight of single living cyanobacterial cells using the Mach-Zehnder double-beam interference microscope. *European Journal of Phyology* **43**:355–364. doi: [10.1080/09670260802168625](https://doi.org/10.1080/09670260802168625).
- Mayo WP**, Elrifi IR, Turpin DH. 1989. The relationship between ribulose biphosphate concentration, dissolved inorganic carbon (DIC) transport and DIC-limited photosynthesis in cyanobacterium *Synechococcus leopoliensis* grown at different concentrations of inorganic carbon. *Plant Physiology* **90**:720–727. doi: [10.1104/pp.90.2.720](https://doi.org/10.1104/pp.90.2.720).
- Miller KR**, Staehelin LA. 1979. Analysis of thylakoid outer surface. Coupling factor is limited to unstacked membrane regions. *The Journal of Cell Biology* **68**:30–47. doi: [10.1083/jcb.68.1.30](https://doi.org/10.1083/jcb.68.1.30).
- Missner A**, Kügler P, Saporov SM, Sommer K, Mathai JC, Zeidel ML, Pohl P. 2008. Carbon dioxide transport through membranes. *The Journal of Biological Chemistry* **283**:25340–25347. doi: [10.1074/jbc.M800096200](https://doi.org/10.1074/jbc.M800096200).
- Omata T**, Price GD, Badger MR, Okamura M, Gohta S, Ogawa T. 1999. Identification of an ATP-binding cassette transporter involved in bicarbonate uptake in the cyanobacterium *Synechococcus* sp strain PCC7942. *Proceedings of the National Academy of Sciences of the United States of America* **96**:13571–13576. doi: [10.1073/pnas.96.23.13571](https://doi.org/10.1073/pnas.96.23.13571).
- Papapostolou D**, Howorka S. 2009. Engineering and exploiting protein assemblies in synthetic biology. *Molecular Biosystems* **5**:723–732. doi: [10.1039/b902440a](https://doi.org/10.1039/b902440a).
- Peña KL**, Castel SE, de Araujo C, Espie GS, Kimber MS. 2010. Structural basis of the oxidative activation of carboxysomal  $\gamma$ -carbonic anhydrase, CcmM. *Proceedings of the National Academy of Sciences of the United States of America* **107**:2455–2460.
- Price G**. 2011. Inorganic carbon transporters of the cyanobacterial CO<sub>2</sub> concentrating mechanism. *Photosynthesis Research* **109**:47–57. doi: [10.1007/s11120-010-9608-y](https://doi.org/10.1007/s11120-010-9608-y).
- Price G**, Badger MR. 1989. Expression of human carbonic anhydrase in the cyanobacterium *Synechococcus* PCC7942 creates a high CO<sub>2</sub>-requiring phenotype. *Plant Physiology* **91**:505–513. doi: [10.1104/pp.91.2.505](https://doi.org/10.1104/pp.91.2.505).
- Price GD**, Badger MR, Woodger FJ, Long BM. 2007. Advances in understanding the cyanobacterial CO<sub>2</sub>-concentrating-mechanism (CCM): functional components, C<sub>i</sub> transporters, diversity, genetic regulation and prospects for engineering into plants. *Journal of Experimental Botany* **58**:1441–1461. doi: [10.1093/jxb/erm112](https://doi.org/10.1093/jxb/erm112).
- Price GD**, Badger MR, Woodger FJ, Long BM. 2008. Advances in understanding the cyanobacterial CO<sub>2</sub>-concentrating-mechanism (ccm): functional components, C<sub>i</sub> transporters, diversity, genetic regulation and prospects for engineering into plants. *Journal of Experimental Botany* **59**:1441–1461. doi: [10.1093/jxb/erm112](https://doi.org/10.1093/jxb/erm112).
- Price GD**, Sultemeyer D, Klughammer B, Ludwig M, Badger MR. 1998. The functioning of the CO<sub>2</sub> concentrating mechanism in several cyanobacterial strains: a review of general physiological characteristics, genes, proteins, and recent advances. *Canadian Journal of Botany* **76**:973–1001. doi: [10.1139/b98-081](https://doi.org/10.1139/b98-081).
- Price GD**, Woodger FJ, Badger MR, Howitt SM, Tucker L. 2004. Identification of a SulP-type bicarbonate transporter in marine cyanobacteria. *Proceedings of the National Academy of Sciences of the United States of America* **101**:18228–18233. doi: [10.1073/pnas.0405211101](https://doi.org/10.1073/pnas.0405211101).
- Reinhold L**, Kosloff R, Kaplan A. 1991. A model for inorganic carbon fluxes and photosynthesis in cyanobacterial carboxysomes. *Canadian Journal of Botany* **69**:984–988. doi: [10.1139/b91-126](https://doi.org/10.1139/b91-126).
- Reinhold L**, Zviman M, Kaplan A. 1989. A quantitative model for inorganic carbon fluxes and photosynthesis in cyanobacterial carboxysomes. *Plant Physiology and Biochemistry: PPB* **27**:945–954.
- Rosgaard L**, de Porcellinis adn JH, Jacobsen AJ, Frigaard NU, Sakuragi Y. 2012. Bioengineering of carbon fixation, biofuels, and biochemicals in cyanobacteria and plants. *Journal of Biotechnology* **162**:137–147. doi: [10.1016/j.jbiotec.2012.05.006](https://doi.org/10.1016/j.jbiotec.2012.05.006).
- Savage DF**, Alfonso B, Chen A, Silver PA. 2010. Spatially ordered dynamics of the bacterial carbon fixation machinery. *Science* **327**:1258–1261. doi: [10.1126/science.1186090](https://doi.org/10.1126/science.1186090).
- Savir Y**, Noor E, Milo R, Tlusty T. 2010. Cross-species analysis traces adaptation of RuBisCO toward optimality in a low-dimensional landscape. *Proceedings of the National Academy of Sciences of the United States of America* **107**:3475–3480. doi: [10.1073/pnas.0911663107](https://doi.org/10.1073/pnas.0911663107).

- Schmid MF**, Paredes AM, Khant HA, Soyer F, Aldrich HC, Chiu W, Shively JM. 2006. Structure of *Halothiobacillus neapolitanus* carboxysomes by cryo-electron tomography. *Journal of Molecular Biology* **364**:526–535. doi: [10.1016/j.jmb.2006.09.024](https://doi.org/10.1016/j.jmb.2006.09.024).
- Shibata M**, Ohkawa H, Kaneko T, Fukuzawa H, Tabata S, Kaplan A, Ogawa T. 2001. Distinct constitutive and low-CO<sub>2</sub>-induced CO<sub>2</sub> uptake systems in cyanobacteria: genes involved and their phylogenetic relationship with homologous genes in other organisms. *Proceedings of the National Academy of Sciences of the United States of America* **98**:11789–11794. doi: [10.1073/pnas.191258298](https://doi.org/10.1073/pnas.191258298).
- Sultemeyer D**, Price GD, Yu JW, Badger MR. 1995. Characterisation of carbon dioxide and bicarbonate transport during steady-state photosynthesis in the marine cyanobacterium *Synechococcus* strain PCC7002. *Planta* **197**:597–607. doi: [10.1007/BF00191566](https://doi.org/10.1007/BF00191566).
- Tcherkez GG**, Farquhar GD, Andrews TJ. 2006. Despite slow catalysis and confused substrate specificity, all ribulose biphosphate carboxylases may be nearly optimized. *Proceedings of the National Academy of Sciences of the United States of America* **103**:7246–7251. doi: [10.1073/pnas.0600605103](https://doi.org/10.1073/pnas.0600605103).
- Tchernov D**, Hassidim M, Luz B, Sukenik A, Reinhold L, Kaplan A. 1997. Sustained net CO<sub>2</sub> evolution during photosynthesis by marine microorganisms. *Current Biology* **7**:723–728. doi: [10.1016/S0960-9822\(06\)00330-7](https://doi.org/10.1016/S0960-9822(06)00330-7).
- Tchernov D**, Silverman J, Luz B, Reinhold L, Kaplan A. 2003. Massive light-dependent cycling of inorganic carbon between oxygenic photosynthetic microorganism and their surroundings. *Photosynthesis Research* **77**:95–103. doi: [10.1023/A:1025869600935](https://doi.org/10.1023/A:1025869600935).
- Volokita M**, Zenvirth D, Kaplan A, Reinhold L. 1984. Nature of the inorganic carbon species actively taken up by the cyanobacterium *Anabaena variabilis*. *Plant Physiology* **76**:599–602. doi: [10.1104/pp.76.3.599](https://doi.org/10.1104/pp.76.3.599).
- Whitehead L**, Long BM, Price GD, Badger MR. 2014. Comparing the *in vivo* function of  $\alpha$ - and  $\beta$ - carboxysomes in two model cyanobacteria. *Plant Physiology* **165**:398–411. doi: [10.1104/pp.114.237941](https://doi.org/10.1104/pp.114.237941).
- Woodger FJ**, Badger MR, Price GD. 2005. Sensing of inorganic carbon limitation in *Synechococcus* PCC7942 is correlated with the size of the internal inorganic carbon pool and involves oxygen. *Plant Physiology* **139**:1959–1969. doi: [10.1104/pp.105.069146](https://doi.org/10.1104/pp.105.069146).
- Yeates TO**, Kerfeld CA, Heinhorst CAK, Cannon GC, Shively JM. 2008. Protein-based organelles in bacteria: carboxysomes and related microcompartments. *Nature Reviews Microbiology* **6**:681–691. doi: [10.1038/nrmicro1913](https://doi.org/10.1038/nrmicro1913).
- Yeates TO**, Tsai TY, Tanaka S, Sawaya MR, Kerfeld CA. 2007. Self-assembly in the carboxysome: a viral capsid-like protein shell in bacterial cells. *Biochemical Society Transactions* **35**:508–511. doi: [10.1042/BST0350508](https://doi.org/10.1042/BST0350508).